Thermoviscoelastic modelling of high strain thin-ply composites by means of multiscale plate and beam models

Orzuri Rique Garaizar*, Su Tian† and Wenbin Yu‡
School of Aeronautics and Astronautics, West Lafayette, IN 47907, USA

Juan M. Fernandez§ and Andrew C. Bergan¶
NASA Langley Research Center, Hampton, VA 23666, USA

High strain thin-ply (HS-TPC) technology is being increasingly adopted for high-performance aerospace applications. Albeit many of these structures such as deployable booms can be modeled as one-dimensional beam problems, there is a lack of themoviscoelastic beam models to efficiently and accurately simulate HS-TPC. This work will use mechanics of structure genome (MSG) to construct linear thermoviscoelastic beam models that can homogenize three-dimensional heterogeneous materials made of constituents with time- and temperature-dependent behavior. The formulation derives the transient strain energy based on integral formulation for thermorheologically simple materials subject to finite temperature changes with the restriction that the strain is small. A lenticular boom is used as a numerical example to verify the MSG-based linear thermoviscoelastic beam model against MSG-based shell/plate model, which has already been validated against experimental data provided by NASA, and direct numerical simulations performed in a finite element commercial package.

I. Introduction

More and more, high-performance aerospace applications such as deployable booms, space antennas [1] or solar sails are relying on high strain thin-ply (HS-TPC) technology. Compared to traditional space-rated metals such as Elgiloy, high strain thin-ply composites demonstrate improved thermal behavior [2] while offering excellent packaging properties, lightweight and low-cost [3, 4]. These structures are designed to operate for long periods of time and withstand certain mechanical loads under wide temperature variations. Polymeric matrices present in composite materials are prone to have time-dependent behavior very sensitive to changes in temperature. The relaxation of the polymeric matrix can indeed lead to an unsuccessful deployment, and their structural integrity, short-term and long-term durability as well as thermal stability are of great concern [2, 5]. The reduction of the bending stiffness and

*Graduate Research Assistant, School of Aeronautics and Astronautics, 1105 Challenger Ave 100, West Lafayette, IN 47906, and AIAA Student Member.
†Graduate Research Assistant, School of Aeronautics and Astronautics, 701 W. Stadium Avenue West Lafayette, IN 47907, and AIAA Member.
‡Professor, School of Aeronautics and Astronautics, 701 W. Stadium Avenue West Lafayette, IN 47907, and AIAA Associate Fellow.
§Research Aerospace Engineering, Structural Dynamics Branch, NASA LaRC, 4 West Taylor Street, Mail Stop 230, and AIAA Member.
¶Research Aerospace Engineering, Durability, Damage Tolerance, and Reliability Branch, NASA LaRC, and AIAA Member.

an incomplete recovery of the structural shape caused by the relaxation of the matrix can compromise the success of the mission for which the structure has been designed for [6, 7] and thus, more accurate models that also account for thermoviscoelastic behavior are necessary.

Many HS-TPC structures such as deployed composite booms can be modeled as beams, thus leading to much simpler governing equations and convenient interpretation of the results. One has to capture the behavior associated with the eliminated two dimensions, described using the cross-sectional coordinates [8], to take advantage of this geometric feature wihile miniizing the loss of accuracy. Bearing in mind its efficiency and simplicity, beam models are often interesting to be used in system level analyses or preliminary designs. Traditional beam models, nonetheless, cannot satisfactorily handle slender structures consisting of highly anisotropic, and heterogeneous materials such as HS-TPCs because these models rely on different ad hoc assumptions such as the uniaxial stress assumption and Euler-Bernoulli assumptions. Fully populated matrix of cross-sectional stiffness properties that capture the couplings among all forms of global deformation and among both in- and out-of-plane components is difficult to be obtain ed using traditional methods [9], and there is a gap between existing linear thermoviscoelastics constitutive models and existing beam models. Most of the research in the linear thermoviscoelastic modelling with beam elements has been focused on the experimental characterization of the bending stiffness [10, 11], using Euler-Bernoulli viscoelastic beam model in draping simulation of textile composites [12] or Timoshenko beam model in frequency domain [13]. Few work has been done in modeling HS-TPC by means of beam models. A recent work by De Zanet and Viquerat [14] is the only attempt of considering Euler-Bernoulli elastic beam models to capture the behavior of HS-TPC that the authors are aware of.

In this work, mechanics of structure genome (MSG) [15] is used to construct an improved linear thermoviscoelastic beam model that allows to homogenize three-dimensional heterogeneous materials made of constituents with time- and temperature-dependent behavior. MSG relies only on the slenderness of the structure and the material and geometric information of the structure, free from ad hoc assumptions and has the potential to be adapted for many constitutive models, yet by making minor changes. It has been extensively demonstrated that the MSG beam model could achieve the same accuracy as 3D direct numerical simulation (DNS) while similar efficiency to traditional beam models [15, 16]. The formulation for the linear viscoelastic constitutive case derives the transient strain energy based on integral formulation for thermorheologically simple materials subject to finite temperature changes with the restriction that the strain is small [17]. The new formulation has been implemented in SwiftComp, a general-purpose multiscale constitutive modeling code based on MSG.

II. MSG-based Linear Thermoviscoelastic Beam Formulation

Following the Boltzmann superposition principle and assuming that there is no strain history prior to $t = 0$ s, the constitutive equation for an anisotropic linear thermoviscoelastic material with non-aging behavior is given by Zocher et al. [18] and Lakes [19] based on the formulation of Schapery [20] as

$$\sigma_{ij}(t) = \int_0^t C_{ijkl}(t-\tau)\dot{\varepsilon}_{kl}(\tau)d\tau \tag{1}$$

where $\sigma_{ij}(t)$ are the instantaneous stress components, t is the time, $C_{ijkl}(t)$ is the stress relaxation stiffness which is a function of time, and $\dot{\varepsilon}_{kl}$ is the strain rate. The term C_{ijkl} represents the fourth-order tensor of relaxation moduli relating stress to strain [18].

MSG-based thermoviscoelastic beam model can be developed considering the 1D Euler-Bernoulli beam model. The kinematics accounts for four time-dependent displacement variables $u_1(t)$, $u_2(t)$, $u_3(t)$, and $\theta_1(t)$ with $u_1(t)$, $u_2(t)$, $u_3(t)$ describing displacements in three directions and $\theta_1(t)$ representing the twist angle, also known as the beam sectional rotation. Thus, the four beam strain measures are defined as [15, 16]

$$\gamma_{11}(t) = \bar{u}_{1,1}(t) \quad \kappa_{11}(t) = \theta_{1,1}(t) \quad \kappa_{12}(t) = -\bar{u}_{3,11}(t) \quad \kappa_{13}(t) = \bar{u}_{2,11}(t) \tag{2}$$

where $\gamma_{11}(t)$ stands for the instantaneous axial strain, and $\kappa_{11}(t)$ denotes the instantaneous twist rate, and $\kappa_{12}(t)$ and $\kappa_{13}(t)$ represent the instantaneous curvatures around x_2 and x_3, respectively. It is noted that the double numbers after comma in the subscript indicate the second derivatives, and $\bar{u}_i$ represents the displacements of the homogenized structure.

The kinetics of 1D Euler-Bernoulli beam model contains four time-dependent stress resultants $F_1(t)$, $M_1(t)$, $M_2(t)$, $M_3(t)$ with $F_1(t)$ denoting the time-dependent axial force, and $M_1(t)$, $M_2(t)$, $M_3(t)$ standing for the time-dependent bending moments about three directions. Let us define $\Gamma(t) = \lfloor \gamma_{11}(t) \;\; \kappa_{11}(t) \;\; \kappa_{12}(t) \;\; \kappa_{13}(t) \rfloor^T$, $\varsigma(t) = \lfloor F_1(t) \;\; M_1(t) \;\; M_2(t) \;\; M_3(t) \rfloor^T$, and the 4×4 beam stiffness matrix $C^b_{ij}(t)$ as

$$C^b(t) = \begin{bmatrix} C^b_{11}(t) & C^b_{12}(t) & C^b_{13}(t) & C^b_{14}(t) \\ C^b_{12}(t) & C^b_{22}(t) & C^b_{23}(t) & C^b_{24}(t) \\ C^b_{13}(t) & C^b_{23}(t) & C^b_{33}(t) & C^b_{34}(t) \\ C^b_{14}(t) & C^b_{24}(t) & C^b_{34}(t) & C^b_{44}(t) \end{bmatrix} \tag{3}$$

Then, Eq. (1) can be rewritten in terms of 1D Euler-Bernouilli beam model as

$$\varsigma(t) = \int_0^t C^b(t-\tau)\dot{\Gamma}d\tau \tag{4}$$

To solve for Eq. (4), similarly to the MSG-based solid case [17, 21] the direct time integration approach that uses a time marching procedure is considered. The constitutive relation can be represented by a recursive form in which the beam stress and strain resultants in the current state are affected by the beam stress resultant history of the previous steps [21, 22]. Thus, the beam stress resultants are computed as

$$\varsigma(t_{n+1}) \equiv \varsigma(t_{n+1}) - \varsigma(t) \tag{5}$$

Let us assume that the terms of $C^b(t)$ are expressed with Prony series as

$$C^b\,(t) = C^b_\infty + \sum_{s_1=1}^{m_1} C^b_s e^{\left(-\frac{t}{\lambda_s}\right)} \tag{6}$$

where C^b_∞ is the long-term beam stiffness matrix, λ_s are the discrete stress relaxation times, and C^b_s stand for the Prony coefficients of the beam stiffness matrix. For the sake of simplicity, the same discrete stress relaxation times are considered for all the components of the 4×4 beam stiffness matrix. It is noted that when time- and temperature-dependent experimental or simulation data is reduced, it is possible to constrain the λ_s in the algorithm to compute the corresponding Prony coefficients.

Furthermore, we approximate the beam strains over the interval Δt_{n+1} (i.e. $t_n \le t \le t_{n+1}$) as

$$\dot{\Gamma}(\tau) = \begin{bmatrix} \dot{\gamma}_{11}(\tau) \\ \dot{\kappa}_{11}(\tau) \\ \dot{\kappa}_{12}(\tau) \\ \dot{\kappa}_{13}(\tau) \end{bmatrix} = \begin{bmatrix} \frac{\partial \gamma_{11}}{\partial \tau} \\ \frac{\partial \kappa_{11}}{\partial \tau} \\ \frac{\partial \kappa_{12}}{\partial \tau} \\ \frac{\partial \kappa_{13}}{\partial \tau} \end{bmatrix} \approx \begin{bmatrix} R_{\gamma_{11_n}} \\ R_{\kappa_{11_n}} \\ R_{\kappa_{12_n}} \\ R_{\kappa_{13_n}} \end{bmatrix} \equiv \begin{bmatrix} \frac{\Delta \gamma_{11}}{\Delta t} \\ \frac{\Delta \kappa_{11}}{\Delta t} \\ \frac{\Delta \kappa_{12}}{\Delta t} \\ \frac{\Delta \kappa_{13}}{\Delta t} \end{bmatrix} \equiv R_{\Gamma_n} \tag{7}$$

where $R_{\gamma_{11_n}}$, $R_{\kappa_{11_n}}$, $R_{\kappa_{12_n}}$ and $R_{\kappa_{13_n}}$ are constants representing beam strain changes over the interval, and R_{Γ_n} is the first-order tensor formed by these constants.

Substituting the approximations given by Eqs. (6)-(7), Eq. (4) can be integrated in a closed form leading to

$$\Delta\varsigma(t_{n+1}) = C^b_{eq}\Delta\Gamma(t_{n+1}) + \Omega^b \tag{8}$$

with

$$
\begin{aligned}
&C^b_{eq} \equiv C^b_\infty + \frac{1}{\Delta t_{n+1}} \sum_{s=1}^{m} \lambda_s C^b_s \left(1 - e^{\frac{-\Delta t_{n+1}}{\lambda_s}}\right) \\
&\Delta\Gamma(t_{n+1}) \equiv R_{\Gamma_{n+1}} \Delta t_{n+1} \\
&\Omega^b \equiv -\sum_{s=1}^{m} \left(1 - e^{\frac{-\Delta t_{n+1}}{\lambda_s}}\right) a_s(t_n)
\end{aligned}
\tag{9}
$$

where $R_{\Gamma_{n+1}}$ is a first-order tensor evaluated for the current time increment, and

$$
a_s(t_n) = e^{\frac{-\Delta t_n}{\lambda_s}} a_s(t_{n-1}) + \lambda_s C^b_s R_{\Gamma_n} \left(1 - e^{\frac{-\Delta t_n}{\lambda_s}}\right) \tag{10}
$$

Finally, for a given beam strain Γ field, it is possible to compute $\Delta\varsigma(t_{n+1})$ with the formulation here presented. Then, $\varsigma(t_{n+1})$ is given as

$$
\varsigma(t_{n+1}) = \varsigma(t_n) + \Delta\varsigma(t_{n+1}) \tag{11}
$$

III. Lenticular Boom Numerical Example

A. High Strain Composite Material

A lenticular boom (CTM) is used as the numerical example to verify the MSG-based linear thermoviscoelastic beam model. A schematic drawing with design parameters is shown in Fig. 1 (a) and the numerical value of the design paramerters is summarized in Table 1. The lenticular boom contains two different HS-TPCs: an MS30/PMT-F7 textile composite and an MR60H/PMT-F7 unidirectional composite. The effective lamina properties of both composite materials have been computed using PMT-F7 resin characterized by NASA and MSG-based solid thermoviscoelastic model that is available in SwiftComp ™ [23]. The fiber constituent properties and microstructure characteristics for the computation have been found in literature (see Ref. [24] for MS30/PMT-F7 and Ref. [9] for MR60H/PMT-F7). Prony coefficients presented in Tables 2-3 have been used to represent the effective viscoelastic properties of both HS-TPC materials at a reference temperature of 40°C. In case of the ply orientation, $[45_{UD}/45_{PW}]$ for both the left and right shells of the lenticular boom is selected.

Table 1 Fixed parameters of the lenticular boom design.

Name	Symbol	Fixed Value
Flattened height	h_f	45 mm
Web height	h_ω	3 mm
Subtended angle	$\alpha_1 = \alpha_2$	90 degree

Table 2 Effective lamina viscoelastic properties of MS30/PMT-F7 textile composite at 40°C.

s	λ_s s	$C_{11,s} = C_{22,s}$ MPa	$C_{12,s}$ MPa	$C_{13,s} = C_{23,s}$ MPa	$C_{33,s}$ MPa	$C_{44,s} = C_{55,s}$ MPa	$C_{66,s}$ MPa
∞		91,526.00	2,856.80	3,070.20	7,285.40	1,975.80	2,020.60
1	3.70E+01	765.69	379.04	447.69	993.64	254.12	266.56
2	1.00E+02	684.27	315.84	376.20	849.00	220.50	230.16
3	1.00E+03	575.65	267.59	318.51	716.91	185.74	194.00
4	5.00E+03	249.90	108.29	130.18	297.08	77.92	81.03
5	1.00E+04	252.27	118.50	140.78	316.55	81.94	85.61
6	5.00E+04	713.04	307.44	370.03	843.80	221.14	229.99
7	1.00E+05	70.53	28.36	34.57	79.42	20.94	21.72
8	5.00E+05	364.46	152.75	184.75	422.85	111.17	115.46
9	1.00E+06	218.08	85.97	105.20	242.39	64.08	66.40
10	5.00E+06	2.34	1.10	1.31	2.96	0.77	0.80

Table 3 Effective lamina viscoelastic properties of MR60H/PMT-F7 unidirectional composite at 40°C.

s	λ_s s	$E_{1,s}$ MPa	$E_{2,s} = E_{3,s}$ MPa	$G_{12,s} = G_{13,s}$ MPa	$G_{23,s}$ MPa	$\nu_{12,s} = \nu_{13,s}$ MPa	$\nu_{23,s}$ MPa
∞		173,790.00	4,954.00	1,721.30	1,676.60	0.259	0.477
1	3.70E+01	555.47	905.26	266.56	254.12	0.000	0.000
2	1.00E+02	144.97	722.78	240.38	240.66	0.000	0.000
3	1.00E+03	107.36	604.62	203.91	202.14	0.000	0.000
4	5.00E+03	93.42	512.56	172.42	171.25	0.000	0.000
5	1.00E+04	34.53	208.97	71.06	70.05	0.000	0.000
6	5.00E+04	41.53	226.57	76.16	75.68	0.000	0.000
7	1.00E+05	99.88	594.68	201.96	199.31	0.000	0.000
8	5.00E+05	9.09	55.59	18.95	18.66	0.000	0.000
9	1.00E+06	48.89	297.03	101.11	99.64	0.000	0.000
10	5.00E+06	27.00	169.06	57.78	56.80	0.000	0.000

B. Full Paper

The full paper will extend the present formulation to also consider non-mechanical stress resultants due to temperature changes. It will also contain the further verification of the MSG-based thermoviscoelastic beam model formulation. To do so, a DNS of the lenticular boom shown in Fig. 1 (b) will be simulated using a finite element commercial package (i.e. Abaqus [25]). This DNS will be considered as the baseline to verify the accuracy of MSG beam model. In these DNS simulations, all the HS-TPC plies are going to be modeled by means of 588,800 linear hexahedral elements of type C3D8. The effective orthotropic viscoelastic lamina properties of the plies will be introduced by means of user-defined mechanical material behavior subroutine (UMAT) [25] in which the three-dimensional hereditary integral is solved by means of a time-marching procedure. This UMAT has already been verified for isotropic viscoelastic materials comparing it against by default material libraries of Abaqus CAE [25] and showed good agreement.

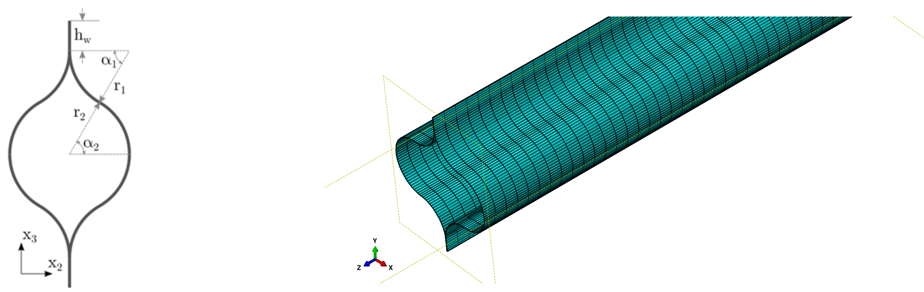

(a) Cross-sectional parameters

(b) Direct numerical simulation (DNS) model

Fig. 1 Lenticular boom design.

In addition, the same formulation are extended to model HS-TPC and the same lenticular boom is modelled by means of MSG-based plate/shell model and solved using shell elements in the same commercial finite element package. For this case, the effective properties of the shell section behavior are defined by means of a user-defined general shell section (UGENS) [25]. We have already validated the MSG-based plate/shell model and the UGENS subroutine against Column Bending Test (CBT) experimental data provided by NASA showing excellent agreement as shown in Fig. 2.

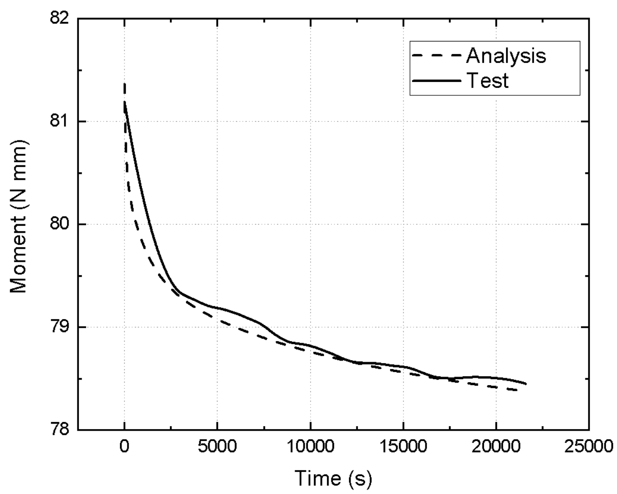

Fig. 2 Validation of the MSG-based plate/shell simulation against CBT experimental data provided by NASA.

In summary, the final paper will verify the MSG-based thermoviscoelastic beam model formulation presented in the previous section against DNS simulations and MSG-based plate/shell model considering for that the lenticular boom as a case study. The efficiency and accuracy of the three models will also be reported.

Funding Sources and Acknowledgments

This research was supported, in part, as part of the Small Business Technology Transfer (STTR) grant from NASA. The authors would like to acknowledge the support of the NASA STTR Phase I: T12.01-3920 (contract number: 80NSSC19C0530). Prof. Wenbin Yu is the co-founder and CTO of AnalySwift, a company that might license a version of a Purdue software code based on the work presented in this article. The views and conclusions obtained herein are those of the authors and should not be interpreted as necessarily representing the official policies or endorsement, either expressed or implied of the funding agency.

The authors also thank the Composites Design and Manufacturing HUB (cdmHUB.org) to provide the cloud platform so that users can easily use the available tools.

References

[1] Yang, Z., Wang, H., Ma, X., Shang, F., Ma, Y., Shao, Z., and Hou, D., "Flexural creep tests and long-term mechanical behavior of fiber-reinforced polymeric composite tubes," *Composite Structures*, Vol. 193, 2018, pp. 154–164. doi:10.1016/j.compstruct.2018.03.083.

[2] Stohlman, O. R., and Loper, E., "Thermal deformation of very slender TRAC booms," *3rd AIAA Spacecraft Structures Conference*, American Institute of Aeronautics and Astronautics, 2016. doi:10.2514/6.2016-1469.

[3] Fernandez, J. M., "Advanced Deployable Shell-Based Composite Booms for Small Satellite Structural Applications Including Solar Sails," *4th International Symposium on Solar Sailing 2017*, 2017.

[4] Fernandez, J. M., Rose, G., Stohlman, O. R., Younger, C. J., Dean, G. D., Warren, J. E., Kang, J. H., Bryant, R. G., and Wilkie, K. W., "An Advanced Composites-Based Solar Sail System for Interplanetary Small Satellite Missions," *2018 AIAA Spacecraft Structures Conference*, American Institute of Aeronautics and Astronautics, 2018. doi:10.2514/6.2018-1437.

[5] Fernandez, J. M., and Murphey, T. W., "A Simple Test Method for Large Deformation Bending of Thin High Strain Composite Flexures," *2018 AIAA Spacecraft Structures Conference*, American Institute of Aeronautics and Astronautics, 2018. doi:10.2514/6.2018-0942.

[6] Mobrem, M., and Adams, D., "Lenticular Jointed Antenna Deployment Anomaly and Resolution Onboard the Mars Express Spacecraft," *Journal of Spacecraft and Rockets*, Vol. 46, No. 2, 2009, pp. 403–410. doi:10.2514/1.36891.

[7] Adamcik, B., Firth, J., Pankow, M., and Fernandez, J. M., "Impact of Storage Time and Operational Temperature on Deployable Composite Booms," *AIAA Scitech 2020 Forum*, American Institute of Aeronautics and Astronautics, 2020. doi:10.2514/6.2020-1183.

[8] Yu, W., Volovoi, V. V., Hodges, D. H., and Hong, X., "Validation of the Variational Asymptotic Beam Sectional Analysis," *AIAA Journal*, Vol. 40, No. 10, 2002, pp. 2105 – 2113.

[9] Lee, A. J., and Fernandez, J. M., "Inducing bistability in Collapsible Tubular Mast booms with thin-ply composite shells," *Composite Structures*, Vol. 225, 2019, p. 111166. doi:10.1016/j.compstruct.2019.111166.

[10] Ropers, S., Kardos, M., and Osswald, T. A., "A thermo-viscoelastic approach for the characterization and modeling of the bending behavior of thermoplastic composites," *Composites Part A: Applied Science and Manufacturing*, Vol. 90, 2016, pp. 22–32. doi:10.1016/j.compositesa.2016.06.016.

[11] Ropers, S., Sachs, U., Kardos, M., and Osswald, T. A., "A thermo-viscoelastic approach for the characterization and modeling of the bending behavior of thermoplastic composites – Part II," *Composites Part A: Applied Science and Manufacturing*, Vol. 96, 2017, pp. 67–76. doi:10.1016/j.compositesa.2017.02.007.

[12] Alshahrani, H., and Hojjati, M., "A theoretical model with experimental verification for bending stiffness of thermosetting prepreg during forming process," *Composite Structures*, Vol. 166, 2017, pp. 136–145. doi:10.1016/j.compstruct.2017.01.030.

[13] Shou, Z., Chen, F., and Yin, H., "Self-heating of a polymeric particulate composite under mechanical excitations," *Mechanics of Materials*, Vol. 117, 2018, pp. 116–125. doi:10.1016/j.mechmat.2017.11.003.

[14] Zanet, G. D., and Viquerat, A., "Thermal response of CFRP deployable tubes in the space environment," *AIAA Scitech 2020 Forum*, American Institute of Aeronautics and Astronautics, 2020. doi:10.2514/6.2020-1439.

[15] Yu, W., "A Unified Theory for Constitutive Modeling of Composites," *Journal of Mechanics of Materials and Structures*, Vol. 11, No. 4, 2016, pp. 379–411.

[16] Liu, X., Yu, W., Gasco, F., and Goodsell, J., "A unified approach for thermoelastic constitutive modeling of composite structures," *Composites Part B: Engineering*, Vol. 172, 2019, pp. 649–659. doi:10.1016/j.compositesb.2019.05.083.

[17] Rique, O., Liu, X., Yu, W., and Pipes, R. B., "Constitutive modeling for time- and temperature-dependent behavior of composites," *Composites Part B: Engineering*, Vol. 184, 2020, p. 107726. doi:10.1016/j.compositesb.2019.107726.

[18] Zocher, M. A., Groves, S. E., and Allen, D. H., "A three dimensional finite element formulation for thermoviscoelastic orthotropic media," *International Journal for Numerical Methods in Engineering*, Vol. 40, No. 12, 1997, pp. 2267–2288. doi:10.1002/(sici)1097-0207(19970630)40:12{$<$}2267::aid-nme156{$>$}3.0.co;2-p.

[19] Lakes, R., *Viscoelastic Materials*, Cambridge University Press, 2009.

[20] Schapery, R. A., "Stress Analysis of Viscoelastic Composite Materials," *Journal of Composite Materials*, Vol. 1, No. 3, 1967, pp. 228–267. doi:10.1177/002199836700100302.

[21] Rique, O., and Yu, W., "Multiscale Modeling of Thermoviscoelasticity for Composite Manufacturing Simulation Using Mechanics of Structure," *AIAA Scitech 2019 Forum*, American Institute of Aeronautics and Astronautics, 2019. doi: 10.2514/6.2019-1203.

[22] Tang, T., and Felicelli, S. D., "Micromechanical investigations of polymer matrix composites with shape memory alloy reinforcement," *International Journal of Engineering Science*, Vol. 94, 2015, pp. 181–194. doi:10.1016/j.ijengsci.2015.05.008.

[23] Yu, W., "SwiftComp™ User Manual - Version 1.2," , 2016. URL `https://cdmhub.org/resources/scstandard/supportingdocs`.

[24] Hamillage, M. Y., Kwok, K., and Fernandez, J. M., "Micromechanical Modeling of High-Strain Thin-Ply Composites," *AIAA Scitech 2019 Forum*, American Institute of Aeronautics and Astronautics, 2019. doi:10.2514/6.2019-1751.

[25] Abaqus, *6.14 Documentation*, Dassault Systèmes Simulia Corporation, 2014.